INT. J. NUM. METH. HEAT FLUID FLOW, VOL. 4, 99–113 (1994)

A MULTIGRID METHOD FOR THE COMPRESSIBLE NAVIER–STOKES EQUATIONS COUPLED TO THE k–ε TURBULENCE EQUATIONS

J. STEELANT AND E. DICK

Department of Mechanical and Thermal Engineering, Universiteit Gent, Sint-Pietersnieuwstraat 41, B-9000 Gent, Belgium

ABSTRACT

The steady compressible Navier–Stokes equations coupled to the k–ε turbulence equations are discretized within a vertex-centered finite volume formulation. The convective fluxes are obtained by the polynomial flux-difference splitting upwind method. The first order accurate part results directly from the splitting. The second order part is obtained by the flux-extrapolation technique using the minmod limiter. The diffusive fluxes are discretized in the central way and are split into a normal and a tangential contribution. The first order accurate part of the convective fluxes together with the normal contribution of the diffusive fluxes form a positive system which allows solution by classical relaxation methods. The source terms in the low-Reynolds k–ε equations are grouped into positive and negative terms. The linearized negative source terms are added to the positive system to increase the diagonal dominance. The resulting positive system forms the left hand side of the equations. The remaining terms are put in the right hand side. A multigrid method based on successive relaxation, full weighting, bilinear interpolation and W-cycle is used. The multigrid method itself acts on the left hand side of the equations. The right hand side is updated in a defect correction cycle.

KEY WORDS Navier–Stokes equations Turbulence Relaxation methods Multigrid methods

INTRODUCTION

In the early developments of two equation models for turbulence, the validation of the models was undertaken on easy geometries such as plane channels and flat plates. The thin layer approximation was then sufficient to describe the physics and the solution could be obtained by the implicit forward marching scheme, originally proposed by Patankar and Spalding[1]. For more complex geometries, the full Navier–Stokes equations must be solved. Basically, two classes of methods for the full Navier–Stokes equations are used nowadays. A first class of methods consists of the explicit time-stepping schemes. An example with Runge–Kutta type stepping, using the Lam–Bremhorst model for the 3D compressible Navier–Stokes is given by Kunz and Lakshminarayana[2]. A second example with a Lax–Wendroff time stepping using the Launder–Sharma model is given by Gerolymos[3]. These methods suffer from a severe time-step restriction due to the presence of the source terms in the turbulence equations. Properly defined implicit time stepping schemes overcome this difficulty. Examples of methods of implicit type are the methods of Vandromme and Ha Minh[4], Yokota[5] and Morrison[6]. The first two of these methods use the central type discretization, the last uses the upwind discretization. Some methods are of hybrid type like the method of Mavriplis and Martinelli[7], where the Navier–Stokes part is solved explicitly and the turbulence part implicitly.

0961–5539/94/020099–15$2.00 *Received June 1993*

Implicit time stepping methods generally allow very large time steps. This observation indicates that it is possible to develop methods that solve directly the steady equations without the use of time stepping. In this paper we develop such a method where the solution is obtained by relaxation and multigrid. To ensure solvability by a relaxation method, the system of discrete equations has to be so-called positive. To obtain positiveness, the different parts of the equations have to be treated carefully: the convective part, the diffusive part and the source part. These three parts have to be split into positive and non-positive contributions. The positive contributions form the left hand side of the system; the non-positive contributions form the right hand side.

The methods of Gerolymos, Yokota and Mavriplis *et al.* employ multigrid. The explicit method of Gerolymos and the hybrid method of Mavriplis *et al.* require implicit residual smoothing since explicit time stepping combined with central discretization cannot provide smoothing. The two foregoing methods use all quantities including k and ε in the multigrid cycle. This causes difficulties in keeping k and ε positive. Therefore some limits on turbulence variables are imposed. By not taking the turbulence quantities into the multigrid cycle, this problem was not encountered by Yokota. In Yokota's method, only the Euler part of the equations is used in the multigrid formulation. It is also limited to high-Reynolds number turbulence equations.

We follow here the approach of Yokota by not taking the turbulence equations into the multigrid cycle. We use, however, the full Navier–Stokes equations in the multigrid cycle. The low-Reynolds number form of the turbulence equations is employed. The efficiency of the method here comes basically from the use of the relaxation method. In a multigrid formulation, relaxation methods are more efficient than those based on time-stepping schemes due to their better smoothing properties.

In this paper, the principles of the method are discussed and are demonstrated on the transitional flat plate geometries T3A and T3B. Different turbulence models are employed to illustrate the universal approach of the relaxation method. The multigrid method is illustrated for one turbulence model.

THE DISCRETIZATION

We consider the set of steady compressible Navier–Stokes equations for turbulent flow, coupled to a k–ε turbulence model. In two dimensions, the Favre-averaged equations take the form:

$$\frac{\partial F}{\partial x}+\frac{\partial G}{\partial y}-\frac{\partial F_v}{\partial x}-\frac{\partial G_v}{\partial y}=S \tag{1}$$

where

$$F=\begin{pmatrix}\rho u\\ \rho uu+p+\frac{2}{3}\rho k\\ \rho uv\\ \rho uE+(p+\frac{2}{3}\rho k)u\\ \rho uk\\ \rho u\varepsilon\end{pmatrix},\quad G=\begin{pmatrix}\rho v\\ \rho uv\\ \rho vv+p+\frac{2}{3}\rho k\\ \rho vE+(p+\frac{2}{3}\rho k)v\\ \rho vk\\ \rho v\varepsilon\end{pmatrix}$$

$$F_v=\begin{pmatrix}0\\ \tau_{xx}\\ \tau_{xy}\\ u\tau_{xx}+v\tau_{xy}+q_x\\ (\mu+\mu_t/\sigma_k)k_x\\ (\mu+\mu_t/\sigma_\varepsilon)\varepsilon_x\end{pmatrix},\quad G_v=\begin{pmatrix}0\\ \tau_{yx}\\ \tau_{yy}\\ u\tau_{yx}+v\tau_{yy}+q_y\\ (\mu+\mu_t/\sigma_k)k_y\\ (\mu+\mu_t/\sigma_\varepsilon)\varepsilon_y\end{pmatrix},\quad S=\begin{pmatrix}0\\ 0\\ 0\\ 0\\ S_k\\ S_\varepsilon\end{pmatrix}$$

The components of the stress tensor τ and the heat flux vector q are given by:

$$\tau_{xx} = (\mu + \mu_t)\left[2\frac{\partial u}{\partial x} - \frac{2}{3}\left(\frac{\partial u}{\partial x} + \frac{\partial v}{\partial y}\right)\right]$$

$$\tau_{xy} = \tau_{yx} = (\mu + \mu_t)\left(\frac{\partial u}{\partial y} + \frac{\partial v}{\partial x}\right)$$

$$\tau_{yy} = (\mu + \mu_t)\left[2\frac{\partial v}{\partial y} - \frac{2}{3}\left(\frac{\partial u}{\partial x} + \frac{\partial v}{\partial y}\right)\right]$$

$$q_x = \left(\frac{\mu}{\mathrm{Pr}} + \frac{\mu_t}{\mathrm{Pr}_t}\right)\frac{\partial h}{\partial x}$$

$$q_y = \left(\frac{\mu}{\mathrm{Pr}} + \frac{\mu_t}{\mathrm{Pr}_t}\right)\frac{\partial h}{\partial y}$$

The molecular viscosity is denoted by μ and the turbulent viscosity by μ_t. Pr is the laminar Prandtl number (taken as 0.71 for air) and Pr_t the turbulent Prandtl number (taken as 0.91 for air). The static enthalpy is denoted by h. E stands for the total internal energy per unit mass:

$$E = \frac{1}{\gamma - 1}\frac{p}{\rho} + \frac{1}{2}u^2 + \frac{1}{2}v^2 + k$$

The source terms of the turbulence model are:

$$S_k = P_k - \rho\varepsilon - \mathscr{D}$$

$$S_\varepsilon = C_{\varepsilon_1} f_1 P_k \frac{\varepsilon}{k} - C_{\varepsilon_2} f_2 \rho \frac{\varepsilon^2}{k} + \mathscr{E}$$

where C_{ε_1}, C_{ε_2}, C_μ, σ_k and σ_ε are the standard k–ε model constants; f_1, f_2 and f_μ are the so-called wall proximity damping functions and $\mathscr{D}$ and $\mathscr{E}$ are the low Reynolds number terms. In the next sections, the discretization of the different parts (convection, diffusion and source) will be discussed and their role in the relaxation method will be detailed.

The convective terms

The convective part is treated by a flux-difference splitting method. Here, the polynomial flux-difference splitting developed by the second author[8] is employed. This method is a variant of Roe-splitting. Using the polynomial character of the convective fluxes F and G with respect to the vector of primitive variables $W^T = \{\rho, u, v, p, k, \varepsilon\}$, differences of flux vectors can be expanded as follows:

$$\Delta F = \begin{bmatrix} \bar{u} & \bar{\rho} & 0 & 0 & 0 & 0 \\ \bar{u}^2 + \frac{2}{3}\overline{k} & \overline{\rho u} + \bar{\rho}\bar{u} & 0 & 1 & \frac{2}{3}\bar{\rho} & 0 \\ \bar{u}\bar{v} & \bar{\rho}\bar{v} & \overline{\rho u} & 0 & 0 & 0 \\ \bar{q}\bar{u} + \frac{5}{3}\overline{k}\bar{u} & a_{42} & \overline{\rho u}\bar{v} & \dfrac{\gamma}{\gamma - 1}\bar{u} & \overline{\rho u} + \frac{2}{3}\bar{\rho}\bar{u} & 0 \\ \overline{k}\bar{u} & \bar{\rho}\overline{k} & 0 & 0 & \overline{\rho u} & 0 \\ \overline{\varepsilon}\bar{u} & \bar{\rho}\overline{\varepsilon} & 0 & 0 & 0 & \overline{\rho u} \end{bmatrix} \Delta W = \mathrm{A}'_1 \Delta W \qquad (2)$$

$$\Delta G = \begin{bmatrix} \bar{v} & 0 & \bar{\rho} & 0 & 0 & 0 \\ \bar{u}\bar{v} & \overline{\rho v} & \bar{\rho}\bar{u} & 0 & 0 & 0 \\ \bar{v}^2 + \frac{2}{3}\bar{k} & 0 & \bar{\rho}\bar{v} + \overline{\rho v} & 1 & \frac{2}{3}\bar{\rho} & 0 \\ \bar{q}\bar{v} + \frac{5}{3}\bar{k}\bar{v} & \overline{\rho v}\bar{u} & a_{43} & \frac{\gamma}{\gamma - 1}\bar{v} & \overline{\rho v} + \frac{2}{3}\bar{\rho}\bar{v} & 0 \\ \bar{k}\bar{v} & 0 & \bar{\rho}\bar{k} & 0 & \overline{\rho v} & 0 \\ \bar{\varepsilon}\bar{v} & 0 & \bar{\rho}\bar{\varepsilon} & 0 & 0 & \overline{\rho v} \end{bmatrix} \Delta W = \mathbf{A}_2' \Delta W \tag{3}$$

where

$$\begin{aligned} \bar{q} &= \tfrac{1}{2}(\overline{u^2} + \overline{v^2}) \\ a_{42} &= \bar{\rho}\bar{q} + \overline{\rho u}\bar{u} + \frac{\gamma}{\gamma - 1}\bar{p} + \bar{\rho}\bar{k} + \frac{2}{3}\overline{\rho k} \\ a_{43} &= \bar{\rho}\bar{q} + \overline{\rho v}\bar{v} + \frac{\gamma}{\gamma - 1}\bar{p} + \bar{\rho}\bar{k} + \frac{2}{3}\overline{\rho k} \end{aligned} \tag{4}$$

The bar denotes the algebraic mean value. Most of the terms in the above expressions are self-evident. Some ambiguity arises in treating the triad terms. The following choices are made. The term ρuu in the momentum equation is seen as the product of the mass flux ρu with the velocity component u. This leads to $\Delta \overline{\rho uu} = \overline{\rho u}\Delta u + \bar{u}\Delta \overline{\rho u} = \overline{\rho u}\Delta u + \bar{u}(\bar{u}\Delta\rho + \bar{\rho}\Delta u)$. The other possible grouping into ρ and u^2 being a density and twice a kinetic energy has no physical meaning.

The energy flux is:

$$\rho uE + \left(p + \frac{2}{3}\rho k\right)u = \frac{1}{\gamma - 1}pu + \frac{1}{2}\rho uu^2 + \frac{1}{2}\rho uv^2 + \rho uk + \left(p + \frac{2}{3}\rho k\right)u$$

The term $\frac{1}{2}\rho uu^2$ is seen as the product of a mass flux ρu with a kinetic energy $\frac{1}{2}u^2$. Similarly, the term ρuk is a product of a mass flux and the turbulence kinetic energy. The term $(p + \frac{2}{3}\rho k)u$ is the product of the effective pressure (molecular plus turbulent pressure) and the velocity u. This means that the groupings in the term $\frac{2}{3}\rho ku$ and the convective term ρuk are different.

The above choice of groupings (i.e. following the physical meaning of the terms) leads to the simplest expressions afterwards. The basic splitting is done with respect to the primitive variables W. A transformation to a splitting with respect to the conservative variables $U^T = \{\rho, \rho u, \rho v, \rho E, \rho k, \rho\varepsilon\}$ is obtained from

$$\Delta U = \begin{bmatrix} 1 & 0 & 0 & 0 & 0 & 0 \\ \bar{u} & \bar{\rho} & 0 & 0 & 0 & 0 \\ \bar{v} & 0 & \bar{\rho} & 0 & 0 & 0 \\ \bar{q} + \bar{k} & \bar{\rho}\bar{u} & \bar{\rho}\bar{v} & \frac{1}{\gamma - 1} & \bar{\rho} & 0 \\ \bar{k} & 0 & 0 & 0 & \bar{\rho} & 0 \\ \bar{\varepsilon} & 0 & 0 & 0 & 0 & \bar{\rho} \end{bmatrix} \Delta W = \mathbf{T}\Delta W$$

The expression $\Delta F = \mathbf{A}_1'\Delta W$ transforms into $\Delta F = \mathbf{A}_1'\mathbf{T}^{-1}\Delta U = \mathbf{A}_1\Delta U$. Similarly $\Delta G = \mathbf{A}_2'\mathbf{T}^{-1}\Delta U = \mathbf{A}_2\Delta U$. The flux-differences are split into a positive and a negative part according

to the sign of the eigenvalues of the matrices $\mathbf{A}_1$ and $\mathbf{A}_2$:

$$\Delta F = \mathbf{A}_1^+ \Delta U + \mathbf{A}_1^- \Delta U$$
$$\Delta G = \mathbf{A}_2^+ \Delta U + \mathbf{A}_2^- \Delta U$$

We consider a vertex-centered finite volume formulation as shown in *Figure 1*. The flux-difference over the surface $s_{1+1/2}$ with length $\Delta s_{i+1/2}$, is:

$$\begin{aligned}\mathscr{F}_{i+1} - \mathscr{F}_i &= (n_x \Delta F_{i,i+1} + n_y \Delta G_{i,i+1})\Delta s_{i+1/2} \\ &= (n_x \mathbf{A}_1 + n_y \mathbf{A}_2)\Delta U_{i,i+1} \Delta s_{i+1/2} \\ &= \mathbf{A}_{i,i+1} \Delta U_{i,i+1} \Delta s_{i+1/2} \\ &= (\mathbf{A}_{i,i+1}^+ + \mathbf{A}_{i,i+1}^-)\Delta U_{i,i+1} s_{i+1/2}\end{aligned}$$

Splitting the matrix A into a positive and negative parts allows the definition of the absolute value of the flux-difference by:

$$|\Delta \mathscr{F}_{i,i+1}| = (\mathbf{A}_{i,i+1}^+ - \mathbf{A}_{i,i+1}^-)\Delta U_{i,i+1} \Delta s_{i+1/2} \tag{5}$$

Based on (5) a first order accurate upwind definition of the flux is:

$$\begin{aligned}\mathscr{F}_{i+1/2} &= \tfrac{1}{2}[\mathscr{F}_i + \mathscr{F}_{i+1} - |\Delta \mathscr{F}_{i,i+1}|] \\ &= \mathscr{F}_i + \Delta s_{i+1/2} \mathbf{A}_{i,i+1}^- \Delta U_{i,i+1}\end{aligned} \tag{5}$$

Fluxes on the other surfaces of the control volume can be written analogously. Summation over the surfaces expresses the inviscid flux balance of a control volume, where the index k denotes the surrounding cells:

$$\sum_k \mathbf{A}_{i,k}^- \Delta U_{i,k} \Delta s_{i,k} = 0$$

or

$$\sum_k \mathbf{A}_{i,k}^- \Delta s_{i,k} (U_k - U_{ij}) = 0$$

or

$$\sum_k (-\mathbf{A}_{i,k}^- \Delta s_{i,k}) U_{i,j} - \sum_k -\mathbf{A}_{i,k}^- \Delta s_{i,k} U_k = 0 \tag{7}$$

Using first order upwind differencing, the convective flux balance has a positive form. This means that the matrix coefficients in (7) have positive eigenvalues. The resulting system can be solved by any relaxation method. The second order correction of the fluxes is constructed by the flux-extrapolation technique involving a minmod limiter. This contribution has no definite character and is therefore placed in the right hand side. Full details on the splitting and the second order correction are given in Reference 8.

The diffusive terms

The treatment of the diffusive terms is illustrated on the momentum-x equation. On the surface $s_{i+1/2}$ of the control volume according to *Figure 1*, the viscous flux terms combine into:

$$n_x \tau_{xx} + n_y \tau_{xy} = (\mu + \mu_t)[n_x(\tfrac{4}{3}u_x - \tfrac{2}{3}v_x) + n_y(u_y + v_x)] \tag{8}$$

The derivatives in (8) are expressed in the local coordinate system (ξ, η):

$$\begin{aligned}u_x &= \frac{1}{J}[\Delta_\xi u \Delta_\eta y - \Delta_\eta u \Delta_\xi y] = g_{11}\Delta_\xi u + g_{12}\Delta_\eta u \\ u_y &= \frac{1}{J}[-\Delta_\xi u \Delta_\eta x + \Delta_\eta u \Delta_\xi x] = g_{21}\Delta_\xi u + g_{22}\Delta_\eta u\end{aligned} \tag{9}$$

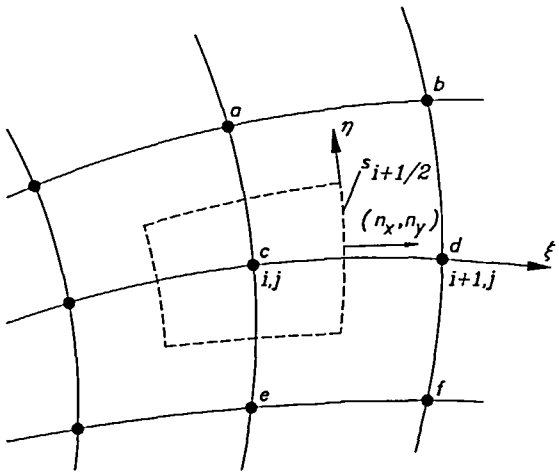

Figure 1 Control volume in the vertex-centered formulation

with $J = \Delta_\xi x \Delta_\eta y - \Delta_\eta x \Delta_\xi y$. For the surface in *Figure 1*:

$$\Delta_\xi u = u_d - u_c, \qquad \Delta_\eta u = \tfrac{1}{4}(u_a + u_b - u_e - u_f)$$

Substitution of (9) in (8) gives:

$$n_x\tau_{xx} + n_y\tau_{xy} = (\mu + \mu_t)[(\tfrac{4}{3}n_x g_{11} + n_y g_{21})\Delta_\xi u + (-\tfrac{2}{3}n_x g_{21} + n_y g_{11})\Delta_\xi v]$$
$$+ (\mu + \mu_t)[(\tfrac{4}{3}n_x g_{12} + n_y g_{22})\Delta_\eta u + (-\tfrac{2}{3}n_x g_{22} + g_{22} + n_y g_{12})\Delta_\eta v]$$

For the other equations, a similar deduction can be made which results in:

$$\mathbf{B}'_\xi \Delta_\xi \tilde{W} + \mathbf{B}'_\eta \Delta_\eta \tilde{W} \tag{10}$$

where $\tilde{W}^T = \{\rho, u, v, e, k, \varepsilon\}$, with e the internal energy.

As the tangential derivatives $\Delta_\eta \tilde{W}$ do not contain the central node, they do not form a positive system and are placed in the right hand side. The normal contribution can be put on the left hand side only if $\mathbf{B}'_\xi$ has positive eigenvalues. To determine these eigenvalues, the matrix $\mathbf{B}'_\xi$ is written as:

$$\mathbf{B}'_\xi = \begin{bmatrix} 0 & 0 & 0 & 0 & 0 & 0 \\ 0 & b_{22} & b_{23} & 0 & 0 & 0 \\ 0 & b_{32} & b_{33} & 0 & 0 & 0 \\ 0 & b_{42} & b_{43} & b_{44} & 0 & 0 \\ 0 & 0 & 0 & 0 & b_{55} & 0 \\ 0 & 0 & 0 & 0 & 0 & b_{66} \end{bmatrix}$$

We see immediately that

$$\lambda_1 = 0$$
$$\lambda_4 = b_{44} = (n_x g_{11} + n_y g_{21})\gamma(\mu/\mathrm{Pr} + \mu_t/\mathrm{Pr}_t)$$
$$\lambda_5 = b_{55} = (n_x g_{11} + n_y g_{21})(\mu + \mu_t/\sigma_k)$$
$$\lambda_6 = b_{66} = (n_x g_{11} + n_y g_{21})(\mu + \mu_t/\sigma_\varepsilon)$$

As $n_x = \Delta_\eta y/\Delta s = \alpha g_{11}$ and $n_y = -\Delta_\eta x/\Delta s = \alpha g_{21}$, where $\alpha > 0$ is a proportionality factor, we have:

$$\lambda_4 = \alpha(g_{11}^2 + g_{21}^2)\gamma(\mu/\mathrm{Pr} + \mu_t/\mathrm{Pr}_t) > 0$$
$$\lambda_5 = \alpha(g_{11}^2 + g_{21}^2)(\mu + \mu_t/\sigma_k) > 0$$
$$\lambda_6 = \alpha(g_{11}^2 + g_{21}^2)(\mu + \mu_t/\sigma_\varepsilon) > 0$$

For the second and third eigenvalues, the submatrix $\mathbf{B}_\xi''$ must be considered:

$$\mathbf{B}_\xi'' = \begin{bmatrix} b_{22} & b_{23} \\ b_{32} & b_{33} \end{bmatrix} = (\mu + \mu_t)\begin{bmatrix} \frac{4}{3}n_x g_{11} + n_y g_{21} & -\frac{2}{3}n_x g_{21} + n_y g_{11} \\ n_x g_{21} - \frac{2}{3}n_y g_{11} & n_x g_{11} + \frac{4}{3}n_y g_{21} \end{bmatrix} \tag{11}$$

With the same proportionality factor the submatrix (11) can be written as:

$$\mathbf{B}_\xi'' = \alpha\frac{(\mu + \mu_t)}{3}\begin{bmatrix} 4g_{11}^2 + 3g_{21}^2 & g_{11}g_{21} \\ g_{11}g_{21} & 3g_{11}^2 + 4g_{21}^2 \end{bmatrix}$$

Eigenvalues of (12) are then:

$$\lambda_2 = \tfrac{4}{3}(\mu + \mu_t)\alpha(g_{11}^2 + g_{21}^2) > 0$$
$$\lambda_3 = (\mu + \mu_t)\alpha(g_{11}^2 + g_{21}^2) > 0$$

The differences in the ξ-direction in the diffusive flux balance form a positive system. The resulting positive system in the left hand side is expressed in the variables $\{\rho, u, v, e, k, \varepsilon\}$. The transformation to the conservative variables is done by

$$\Delta U = \begin{bmatrix} 1 & 0 & 0 & 0 & 0 & 0 \\ \bar{u} & \bar{\rho} & 0 & 0 & 0 & 0 \\ \bar{v} & 0 & \bar{\rho} & 0 & 0 & 0 \\ \bar{q} + \bar{k} + \bar{e} & \bar{\rho}\bar{u} & \bar{\rho}\bar{v} & \bar{\rho} & \bar{\rho} & 0 \\ \bar{k} & 0 & 0 & 0 & \bar{\rho} & 0 \\ \bar{\varepsilon} & 0 & 0 & 0 & 0 & \bar{\rho} \end{bmatrix}\Delta\tilde{W} = \tilde{\mathbf{T}}\Delta\tilde{W}$$

To transform we use $\Delta\tilde{W} = \tilde{\mathbf{T}}^{-1}\Delta U$.

On the surface $s_{i+1/2}$, the contribution of the diffusive flux is:

$$\mathbf{B}_\xi\tilde{\mathbf{T}}^{-1}\Delta_\xi U_{i,i+1} + \mathbf{B}_\eta'\tilde{\mathbf{T}}^{-1}\Delta_\eta U_{i,i+1}]\Delta s_{i+1/2} = [\mathbf{B}_\xi\Delta_\xi U_{i,i+1} + \mathbf{B}_\eta\Delta_\eta U_{i,i+1}]\Delta s_{i+1/2}$$

By summing the viscous fluxes and subtracting the result from expression (7), we obtain

$$\left[\sum_k(-\mathbf{A}_{i,k}^- + \mathbf{B}_{\xi,i,k})\Delta s_{i,k}\right]U_{ij} - \sum_k(-\mathbf{A}_{i,k}^- + \mathbf{B}_{\xi,i,k})\Delta s_{l,k}U_k = \sum_k \mathbf{B}_{\eta,i,k}\Delta\mathbf{s}_{i,k}\Delta_\eta U_{i,k} \tag{13}$$

In a relaxation method, the central node on the left hand side is brought at the new iteration level $(n + 1)$ while the neighbouring nodes are at the old or the new level, depending on the method. For Jacobi-relaxation, equation (13) can be written into Δ-formulation by

$$\left[\sum_k(-\mathbf{A}_{i,k}^- + \mathbf{B}_{\xi,i,k})\Delta s_{i,k}\right](U_{ij}^{n+1} - U_{ij}^n) = \sum_k(-\mathbf{A}_{i,k}^- + \mathbf{B}_{\xi,i,k})\Delta s_{i,k}(U_k^n - U_{i,j}^n)$$
$$+ \sum_k \mathbf{B}_{\eta,i,k}\Delta\mathbf{s}_{i,k}\Delta_\eta\mathbf{U}_{i,k}^n \tag{14}$$

For Gauss–Seidel relaxation, some terms in the right hand side of (14) are at the new level, depending on the ordering of relaxation.

The source terms

Whereas the construction of the convective and diffusive Jacobians is rather straightforward, this is not the case for the source terms. For the source terms, a proper linearization must be chosen. The Jacobian of the negative source terms is then to be brought into the left-hand side to increase the diagonal dominance of the system of equations, see Vandromme[9]. Dependent on the k–ε-model, a different linearization is necessary. Until now the flux balance of the control volume is, with $\Omega_{i,j}$ the volume:

$$\sum_k (-\mathbf{A}^-_{i,k} + \mathbf{B}_{\xi,i,k})\Delta s_{i,k}(U^{n+1}_{ij} - U^n_{i,j}) = \text{RHS} + S\Omega_{i,j}$$

The source term S is split into positive and negative terms that are placed at a different iteration level:

$$S = S^n_+ + S^{n+1}_- = S^n_+ + S^n_- + \frac{\partial S^-}{\partial U}(U^{n+1}_{ij} - U^n_{ij})$$

Finally we obtain:

$$\left[\sum_k (-\mathbf{A}^-_{i,k} + \mathbf{B}_{\xi,i,k})\Delta s_{i,k} - \frac{\partial S^-}{\partial U}\Omega_{i,j}\right](U^{n+1}_{ij} - U^n_{ij}) = \text{RHS} + (S^n_+ + S^n_-)\Omega_{i,j}$$

Source terms of a k–ε model can be written as:

$$S_k = P_k - \rho\varepsilon - \mathscr{D}$$

$$S_\varepsilon = [C_{\varepsilon_1} f_1 P_k - C_{\varepsilon_2} f_2 \rho\varepsilon]\frac{1}{\mathscr{T}} + \mathscr{E}$$

with

$$\begin{aligned} \mathscr{T} &= k/\varepsilon \\ P_k &= \left[\mu_t\left(\frac{\partial u_i}{\partial x_j} + \frac{\partial u_j}{\partial x_i} - \frac{2}{3}\delta_{ij}\frac{\partial u_k}{\partial x_k}\right) - \frac{2}{3}\delta_{ij}\rho k\right]\frac{\partial u_i}{\partial x_j} \\ \mu_t &= C_\mu f_\mu \rho k \mathscr{T} \end{aligned} \tag{15}$$

In our study, 3 models are compared: the Launder–Sharma model (LS)[10], the Lam–Bremhorst model (LB) with the modification of Sieger *et al.*[11] and the Yang–Shih model (YS)[12]. The five basic constants are $C_\mu = 0.09$, $C_{\varepsilon_1} = 1.44$, $C_{\varepsilon_2} = 1.92$, $\sigma_k = 1$, $\sigma_\varepsilon = 1.3$.

Table 1 summarizes the low Reynolds terms together with the boundary conditions for these models and *Table 2* gives the damping functions.

Table 1 Low Reynolds terms

k–ε	$\mathscr{T}$	ε_w – B.C.	$\mathscr{D}$	$\mathscr{E}$
LS	$\frac{k}{\varepsilon}$	0	$2\mu\left(\frac{\partial\sqrt{k}}{\partial y}\right)^2$	$2\mu\nu_t\left(\frac{\partial^2 u}{\partial y^2}\right)^2$
LB	$\frac{k}{\varepsilon}$	$\frac{\partial\varepsilon}{\partial y} = 0$	0	0
YS	$\frac{k}{\varepsilon} + \sqrt{\frac{\nu}{\varepsilon}}$	$2\mu\left(\frac{\partial\sqrt{k}}{\partial y}\right)^2$	0	$\mu\nu_t\left(\frac{\partial^2 u}{\partial y^2}\right)^2$

Table 2 Damping functions

k–ε	f_μ	f_1	f_2
LS	$\exp\left[\frac{-3.4}{(1+R_T/50)^2}\right]$	1	$1-0.3\exp(-R_T^2)$
LB	$[1-\exp(-0.0165R_y)]^2\left(1+\frac{20.5}{R_T}\right)$	$1+\left(\frac{0.05}{f_\mu}\right)^3$	$1-\exp(-R_T^2-10^{-10})$
YS	$[1-\exp(-a_1R_y-a_3R_y^3-a_5R_y^5)]^{1/2}$	1	$1-0.22\exp\left(-\frac{R_T^2}{36}\right)$

$$R_T=\frac{k}{\nu\tau}\,R_y=\frac{\sqrt{k}y}{\nu}\,a_1=1.5\times10^{-4},a_3=5.0\times10^{-7},a_5=1.0\times10^{-10}$$

The negative source terms taken into consideration for linearization are the same for all models:

$$S_k^- = -\rho\varepsilon - \mathscr{D}$$
$$S_\varepsilon^- = -C_{\varepsilon_2}f_2\rho\varepsilon\frac{1}{\mathscr{T}} \tag{16}$$

For simplicity, we consider first the LS and LB model. By use of (15) and *Table 1*, expressions (16) can be altered into:

$$S_k^- = -\left[\frac{C_\mu f_\mu}{\mu_t}\right](\rho k)^2-\left[\frac{\mathscr{D}}{\rho k}\right]\rho k$$
$$S_\varepsilon^- = -[C_{\varepsilon_2}f_2]\frac{(\rho\varepsilon)^2}{\rho k} \tag{17}$$

If, following Vandromme[9], the quantities in square brackets are considered to be constant, a possible linearization which guarantees positiveness, is:

$$\frac{\partial(S_k^-;S_\varepsilon^-)}{\partial(\rho k;\rho\varepsilon)}=\begin{bmatrix}\frac{\partial S_k^-}{\partial\rho k} & \frac{\partial S_k^-}{\partial\rho\varepsilon}\\ \frac{\partial S_\varepsilon^-}{\partial\rho k} & \frac{\partial S_\varepsilon^-}{\partial\rho\varepsilon}\end{bmatrix}=\begin{bmatrix}-\frac{2C_\mu f_\mu}{\mu_t}(\rho k)-\frac{\mathscr{D}}{\rho k} & 0\\ C_{\varepsilon_2}f_2\left(\frac{\rho\varepsilon}{\rho k}\right)^2 & -2C_{\varepsilon_2}f_2\frac{\rho\varepsilon}{\rho k}\end{bmatrix}$$

For the YS model, the same combinations are kept constant, but due to the formulation of $\mathscr{T}$, this results in a more complex Jacobian:

$$\frac{\partial(S_k^-;S_\varepsilon^-)}{\partial(\rho k;\rho\varepsilon)}=\begin{bmatrix}-\frac{(\sqrt{\nu}+\sqrt{\nu+4k\mathscr{T}})^2}{2k\mathscr{T}^2} & 0\\ C_{\varepsilon_2}f_2\frac{1}{\mathscr{T}^2} & -C_{\varepsilon_2}f_2\left(2\mathscr{T}-\frac{1}{2}\sqrt{\frac{\nu}{\varepsilon}}\right)\frac{1}{\mathscr{T}^2}\end{bmatrix}$$

TRANSITION RESULTS

Transitional flow with a zero-pressure gradient was calculated over a flat plate with a freestream level of 3% (Case T3A) and 6% (Case T3B) respectively. These test cases are described by Savill[13]. A stretched grid of 385 × 97 points was used. The grid extends upstream of the plate, with the sharp leading edge at station 97. The first grid point in the direction normal to the plate lies at about $y^+ = yu_\tau/\nu = 1$, where u_τ is the friction velocity. Stretching was applied normal

to the plate and in the flow direction near the leading edge. A detail of the grid in the leading edge region is shown in *Figure 2*.

Uniform inlet profiles for total temperature, total pressure, k and ε were specified. At inlet, Mach number was extrapolated from the flow field. The values of k and ε at the inlet were calculated with the equations for k and ε for uniform flow with velocity U:

$$U\frac{\partial k}{\partial x} = -\varepsilon$$

$$U\frac{\partial \varepsilon}{\partial x} = -C_{\varepsilon_2}\frac{\varepsilon^2}{k}$$

where at the leading edge the following values were matched to be in accordance with the experiments[12,13], for L = 1 m:

$$k_e = \tfrac{3}{2}(0.03U_e)^2, \qquad \frac{\varepsilon_e}{U_e^3/L} = 2.86 \times 10^{-3}, \qquad U_e = 5.2 \text{ m/s (T3A)}$$

$$k_e = \tfrac{3}{2}(0.06U_e)^2, \qquad \frac{\varepsilon_e}{U_e^3/L} = 1.22 \times 10^{-2}, \qquad U_e = 9.6 \text{ m/s (T3B)}$$

The upper and right boundaries are outlet boundaries. There, pressure was imposed. Velocity components, temperature and turbulent quantities were extrapolated. The part of the lower boundary upstream of the leading edge was treated as a symmetry line. At the plate, no-slip and adiabatic boundary conditions were imposed. Density and pressure were obtained by characteristic combinations of the equations[8].

The results were obtained with Gauss–Seidel relaxation. The precise procedure is described in the next paragraph. *Figure 3* shows the distribution of the skin friction coefficient for the T3A case and all three models. *Figure 4* shows the same result for the T3B case with the YS-model. The upper and lower lines correspond with fully laminar and fully turbulent flow fields.

Transition point and transition length are not well predicted by all models, when compared to experimental results[13]. This shows that the models still have to be much improved. The calculated k-profiles for the LS-model (*Figure 5*) and LB-model do not reach the correct level. Only the YS-model is able to obtain the peak values of $k^+ \approx 4$ to 5 near the wall (*Figure 6*). This is probably due to the elimination of the singularities near the wall of the k–ε model in

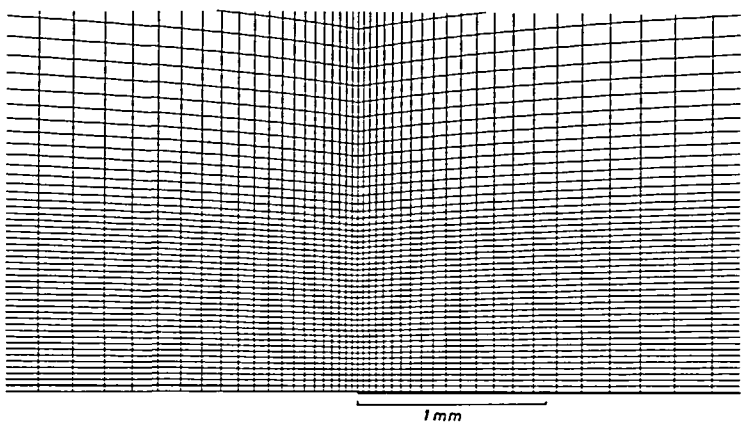

Figure 2 Detail of the grid near the leading edge

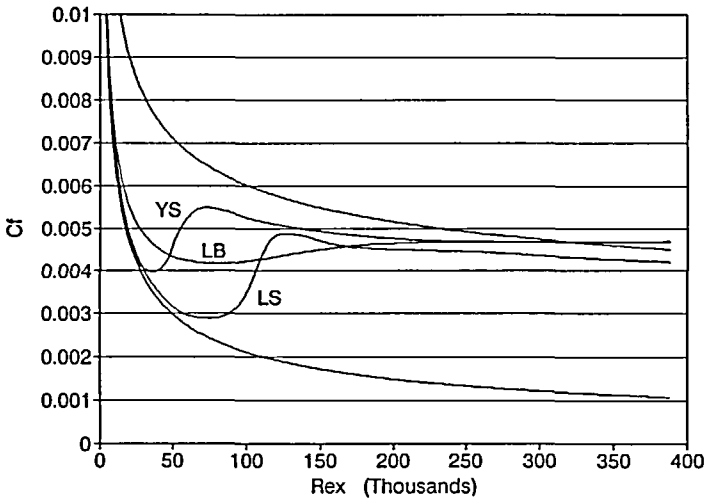

Figure 3 Skin friction for Case T3A

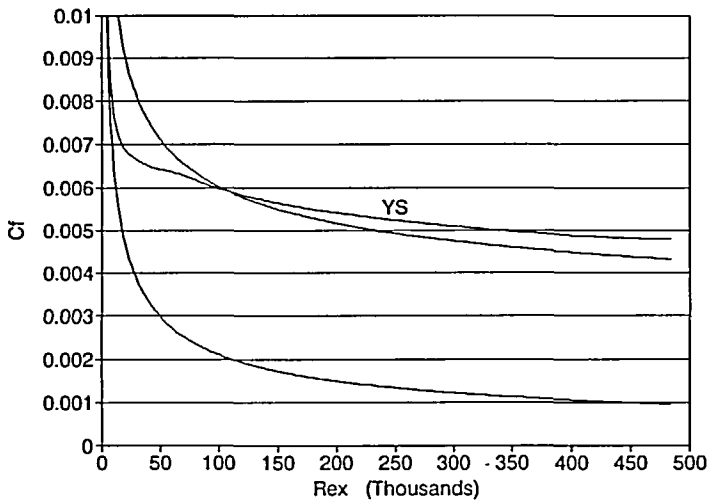

Figure 4 Skin friction for Case T3B

the YS-version. So, the YS-model seems to be the most promising. We do not enter here a discussion of the modifications to the model necessary to obtain better predictions in transitional flows. This will be the subject of future work. The profiles shown in *Figure 5* and *Figure 6* are at the position $Re_x = 3600, 51500, 105750, 163000, 222500, 283500$.

MULTIGRID FORMULATION

A standard multigrid method using four grids (385 × 97; 193 × 49; 97 × 25; 49 × 13), *W*-cycle, full weighting as restriction for residuals and bilinear interpolation as prolongation, was employed. Three lexicographic Gauss–Seidel relaxations with underrelaxation factor 0.9 were used as prerelaxation and as postrelaxation. The first relaxation starts from the left bottom point

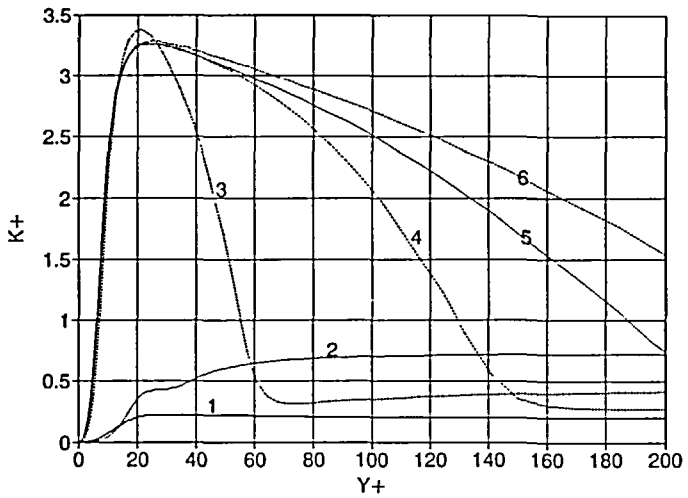

Figure 5 k-Profiles for LS-model, Case T3A

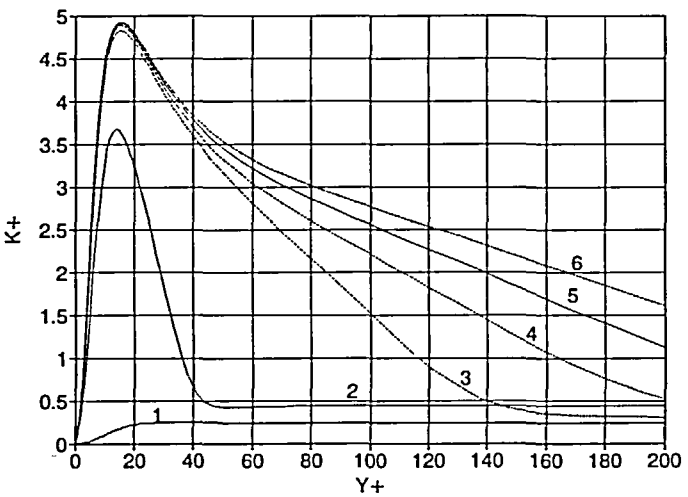

Figure 6 k-Profiles for YS-model, Case T3A

and ends at right upper point. The second relaxation has the reversed ordering. The third relaxation has the same ordering as the first one. The multigrid acts on the left hand side of the set of equations. The right hand side is updated with a defect correction cycle. The procedure is the same as the one used by the second author for the Euler equations in Reference 8, except for the ordering of the relaxation.

Figure 7 shows the cycle configuration. The operation count is indicated. A relaxation on the current grid is taken as one local work unit. A residual evaluation plus the associated grid transfer is also taken as one local work unit. The 1 + 3 + 1 in *Figure 7* stands for the construction of the right hand side of the coarse grid equations, three relaxations and one residual evaluation. The update of the right hand side of the system of equations in the defect correction is also taken as one work unit. The cost of the cycle is 14.0625 work units on the finest level. This was verified against actual computing times.

The calculation starts from uniform flow. First a laminar solution is calculated up to a sufficient level of convergence. With this solution, initial values of k and ε are calculated according to the boundary layer laws[13]:

$$k = k_i\left(\frac{u}{u_i}\right)^2 \qquad \varepsilon = 0.3k\frac{\partial u}{\partial y} \qquad \text{with} \quad \varepsilon \geqslant \varepsilon_i$$

where the subscript i refers to inlet conditions.

The turbulence equations are solved only on the finest grid and are not taken into the multigrid cycle. So, the same multigrid procedure as for the laminar starting phase is employed. This means that the turbulent viscosity is constant during a multigrid cycle and is only updated at the finest grid.

Figure 8 shows the convergence behaviour for the T3A case, using the YS-model. The residual shown is the maximum residual over all equations and all nodes on the finest grid at the end of the cycle. In the figures the comparison is made with a single grid calculation. There, three relaxations were performed before the right hand side of the equations was updated. So, the single grid calculation also uses the defect correction principle. Each defect correction cycle is counted as 4 work units. *Figure 9* shows the same result for the T3B case.

The convergence behaviour of the single grid and multigrid calculations is similar in form. For example, for the T3A case, both convergence histories show a stagnation phase. There is no clear explanation for this phenomenon. It is not seen in the convergence history of the T3B case. For both cases, the final convergence is much deeper in the multigrid formulation than in the single grid formulation.

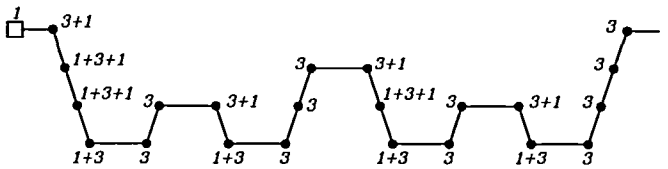

Figure 7 The multigrid cycle; □ = defect correction

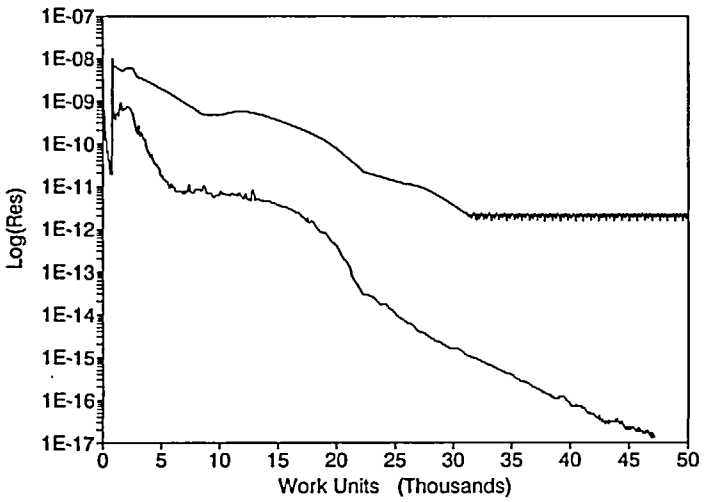

Figure 8 Convergence of single grid and multigrid calculations for the Case T3A; YS-model

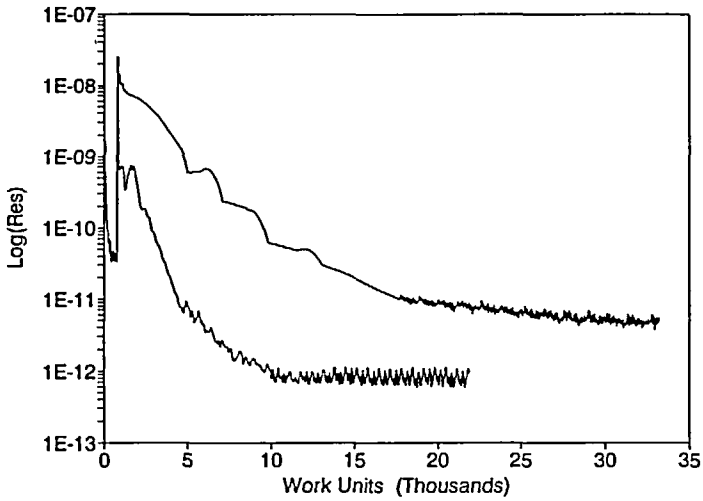

Figure 9 Convergence of sijgle grid and multigrid calculations for the Case T3B; YS-model

The gain of the multigrid method with respect to the single grid method increases, as is typical, with convergence level. For the T3A case, the gain is not very big due to the stagnation phenomenon. It is of the order of 2. For the T3B case, the gain is about 3.4 for the convergence level 10^{-10} and about 4.1 for the convergence level 10^{-11}. Final convergence for the T3B case is obtained in multigrid form after about 10000 work units. The T3A case requires more than 40000 work units but converges deeper. Of course, final convergence is not necessary to obtain usable results. For both the T3A and T3B cases, plotted results obtained at a convergence level of 10^{-10} cannot be distinguished from the results at final convergence. The convergence level of 10^{-10} is reached after about 4000 work units for the T3A case and after about 3000 work units for the T3B case. The convergence speed of the multigrid method is comparable to the speed of the methods of Gerolymos[3] and Mavriplis *et al.*[7], who use also the low-Reynolds form of the turbulence equations. The same speed is obtained here although in the present method the turbulence equations are not taken into the multigrid cycle. Furthermore, the test cases used here are to be considered as very demanding on the convergence due to the transitional character of the flow. The examples used by Gerolymos and Mavriplis *et al.* are fully turbulent and do not have this difficulty.

CONCLUSION

A relaxation method for the steady Navier–Stokes equations coupled to the low-Reynolds number k–ε equations was developed. It was shown that the steady problem can be solved without recourse to time-stepping. The relaxation method was employed in a multigrid formulation. The turbulence equations are not taken into the multigrid cycle. The method was applied to two transitional flow test cases. Considering the difficulty of the test cases, the obtained speed of convergence is very good.

ACKNOWLEDGEMENT

The research reported here was granted under contract 9.0001.91 by the Belgian National Science Foundation Foundation (N.F.W.O.) and under contract IUAP/17 as part of the Belgian National

Programme on Interuniversity Poles of Attraction, initiated by the Belgian State, Prime Minister's Office, Science Policy Programming.

REFERENCES

1 Patankar, S. V. and Spalding, D. B. A calculation procedure for heat, mass and momentum transfer in three-dimensional parabolic flows, *J. Heat Mass Transfer*, **15**, 1787–1806 (1971)
2 Kunz, R. F. and Lakshminarayana, B. Three-dimensional Navier–Stokes computation of turbomachinery flows using an explicit numerical procedure and a coupled k–ε turbulence model, *J. of Turbomachinery*, **114**, 627–642 (1992)
3 Gerolymos, G. A. Implicit multiple-grid solution of the compressible Navier–Stokes equations using k–ε turbulence closure, *AIAA J.*, **28**, 1707–1717 (1990)
4 Vandromme, D. and Ha Minh, H. About the coupling of turbulence closure models with averaged Navier–Stokes equations, *J. of Computational Physics*, **65**, 386–409 (1986)
5 Yokota, J. W. Diagonally inverted lower-upper factored implicit multigrid scheme for the three-dimensional Navier–Stokes equations, *AIAA J*, **28**, 1642–1649 (1990)
6 Morrison, J. H. A compressible Navier–Stokes solver with two-equation and Reynolds stress turbulence closure models, *NASA Contractor Report 4440* (1992)
7 Mavriplis, D. J. and Martinelli, L. Multigrid solution of compressible turbulent flow on unstructured meshes using a two-equations model, *NASA Contractor Report 187513*
8 Dick, E. Multigrid solution of steady Euler equations based on polynomial flux-difference splitting, *Int. J. Num. Methods Heat Fluid Flow*, **1**, 51–62 (1991)
9 Vandromme, D. Turbulence modeling for compressible flows and implementation in Navier–Stokes solvers, *VKI-LS 1991-02* (1991)
10 Patel, V. C., Rodi, W. and Scheuerer, G. Turbulence models for near-wall and low Reynolds number flows: a review, *AIAA J.*, **23**, 1308–1319 (1984)
11 Sieger, K., Schulz, A., Crawford, M. E. and Wittig, S. Comparative study of low-Reynolds number k–ε turbulence models for predicting heat transfer along turbine blades with transition, *Proc. Int. Symp. Heat Transfer in Turbomachinery*, Athens (1992)
12 Yang, Z. and Shih, T. H. A k–ε calculation of transitional boundary layers, *ICOMP-92-08* (1992)
13 Savill, A. M. A synthesis of T3 test case predictions, in *Num. Simulation of Unsteady Flows and Transition to Turbulence* (Eds. O. Pironneau *et al.*), Cambridge University Press, 404–442 (1992)